RBM ONLINE

ELSEVIER

Article

Optimizing bone morphogenic protein 4-mediated human embryonic stem cell differentiation into trophoblast-like cells using fibroblast growth factor 2 and transforming growth factor-β/activin/nodal signalling inhibition

Mariann Koel [a,b,c,*], ***Urmo Võsa*** [d], ***Kaarel Krjutškov*** [a,c,e], ***Elisabet Einarsdottir*** [c,e], ***Juha Kere*** [c,e], ***Juha Tapanainen*** [f], ***Shintaro Katayama*** [c], ***Sulev Ingerpuu*** [b], ***Viljar Jaks*** [b,g], ***Ulf-Hakan Stenman*** [h], ***Karolina Lundin*** [f], ***Timo Tuuri*** [f], ***Andres Salumets*** [a,f,i,j]

[a] *Competence Centre on Health Technologies, Tartu, Estonia*
[b] *Department of Cell Biology, Institute of Molecular and Cell Biology, University of Tartu, Tartu, Estonia*
[c] *Department of Biosciences and Nutrition, and Centre for Innovative Medicine, Karolinska Institutet, Huddinge, Sweden*
[d] *Estonian Genome Center, University of Tartu, Tartu, Estonia*
[e] *Molecular Neurology Research Program, University of Helsinki and Folkhälsan Institute of Genetics, Helsinki, Finland*
[f] *Department of Obstetrics and Gynecology, University of Helsinki and Helsinki University Hospital, Helsinki, Finland*
[g] *Department of Biosciences, Karolinska Institutet, Huddinge, Sweden*
[h] *Department of Clinical Chemistry, University of Helsinki, Helsinki, Finland*
[i] *Department of Obstetrics and Gynaecology, University of Tartu, Tartu, Estonia*
[j] *Institute of Biomedicine and Translational Medicine, University of Tartu, Tartu, Estonia*

Mariann Koel obtained her MSc in Cell Biology from the University of Tartu (cum laude, 2013) and she is continuing her PhD studies at the same university. Currently she is working as a researcher at the Competence Centre on Health Technologies in Estonia. Her research interests are related to trophoblast differentiation, endometrium receptivity and embryo implantation.

KEY MESSAGE

FGF2 inhibition accelerates and TGF-β/activin/nodal inhibition decreases BMP4 mediated differentiation of syncytiotrophoblasts from hESC. Furthermore, inhibition of FGF2 is a major trigger for the production of hyperglycosylated HCG. This knowledge enables us to find an optimal model for studying the early development of human trophoblasts in normal and complicated pregnancy.

* Corresponding author.
E-mail address: mariannkoel@gmail.com (M Koel).
http://dx.doi.org/10.1016/j.rbmo.2017.06.003

ABSTRACT

Several studies have demonstrated that human embryonic stem cells (hESC) can be differentiated into trophoblast-like cells if exposed to bone morphogenic protein 4 (BMP4) and/or inhibitors of fibroblast growth factor 2 (FGF2) and the transforming growth factor beta (TGF-β)/activin/nodal signalling pathways. The goal of this study was to investigate how the inhibitors of these pathways improve the efficiency of hESC differentiation when compared with basic BMP4 treatment. RNA sequencing was used to analyse the effects of all possible inhibitor combinations on the differentiation of hESC into trophoblast-like cells over 12 days. Genes differentially expressed compared with untreated cells were identified at seven time points. Additionally, expression of total human chorionic gonadotrophin (HCG) and its hyperglycosylated form (HCG-H) were determined by immunoassay from cell culture media. We showed that FGF2 inhibition with BMP4 activation up-regulates syncytiotrophoblast-specific genes (*CGA*, *CGB* and *LGALS16*), induces several molecular pathways involved in embryo implantation and triggers HCG-H production. In contrast, inhibition of the TGF-β/activin/nodal pathway decreases the ability of hESC to form trophoblast-like cells. Information about the conditions needed for hESC differentiation toward trophoblast-like cells helps us to find an optimal model for studying the early development of human trophoblasts in normal and in complicated pregnancy.

Introduction

The first cell fate decision in mammalian development is the segregation of the trophectoderm and the inner cell mass that leads to blastocyst formation. During human embryo implantation, the outer trophectoderm layer attaches to the endometrial epithelial cells and differentiates into villous cyto- and syncytiotrophoblasts which, in combination with extravillous trophoblast (EVT) cells, are required for the formation of a functional placenta. Several studies have demonstrated that human embryonic stem cells (hESC) can be directed to differentiate into trophoblast cells if exposed to the transforming growth factor **beta** (TGF-β) superfamily member bone morphogenetic protein 4 (BMP4) (Amita et al., 2013; Chen et al., 2013; Das et al., 2007; Erb et al., 2011; Li et al., 2013; Marchand et al., 2011; Sudheer et al., 2012; Telugu et al., 2013; Xu et al., 2002; Yabe et al., 2016; Yang et al., 2015). However, it is known that bone morphogenic proteins (BMP) are able to induce differentiation not only into trophoblast cells, but also into embryonic lineages (mesoderm and endoderm) (Teo et al., 2012; Zhang et al., 2008). To prevent the formation of other cell lineages and to produce a more homogenous trophoblast cell population, the inhibition of fibroblast growth factor 2 (FGF2) and TGF-β/activin/nodal signalling pathways in combination with BMP4 treatment have recently been utilized (Amita et al., 2013; Lee et al., 2015; Sudheer et al., 2012).

The TGF-β/activin/nodal and FGF2 signalling pathways are major components that support hESC self-renewal (Vallier et al., 2005). TGF-β/activin/nodal ligands belong to the TGF-β superfamily that also includes members of the BMP family. These two branches of the TGF-β/BMP signalling pathways, BMP and TGF-β/activin/nodal signalling, normally antagonize each other, partly because they need to compete for the common factor SMAD4, which is required for the activation of both branches (**Figure 1A**). FGF2 has been shown to inhibit the BMP4-directed differentiation of hESC (Das et al., 2007), or even switch it toward mesendodermal differentiation, characterized by a uniform expression of T (brachyury) and other primitive streak markers (Yu et al., 2011). FGF2 signal inhibition inversely directs BMP4-mediated differentiation of hESC to human chorionic gonadotrophin (HCG)-producing syncytiotrophoblasts (Sudheer et al., 2012; Yu et al., 2011).

Several independent studies have previously utilized BMP4 with or without FGF2 and/or TGF-β/activin/nodal signalling inhibitors to differentiate hESC into trophoblastic cells (Amita et al., 2013; Chen et al., 2013; Das et al., 2007; Erb et al., 2011; Li et al., 2013, p. 4; Lichtner et al., 2013; Marchand et al., 2011; Shirley et al., 2012; Sudheer et al., 2012; Telugu et al., 2013; Xu et al., 2002). However, the individual molecular effect of BMP4 induction and FGF2 and/or TGF-β/activin/nodal inhibition is still not known. Therefore, the aim of the current study was to investigate the individual effects and potential co-action between FGF2 and TGF-β/activin/nodal pathway inhibition on trophoblast differentiation. To obtain a deeper insight into the biological effects of the aforementioned inhibitors, full transcriptome analysis by RNA sequencing (RNA-seq) was used to describe the changes in gene expression during BMP4-activated differentiation.

Materials and methods

Cell culture

The pluripotent hESC line H9 (WiCell Research Institute, Madison, WI, USA) was cultured on a growth factor-reduced Matrigel® coating (BD Biosciences, Bedford, UK) in StemPro medium (Life Technologies, Carlsbad, CA, USA). For trophoblast-directed differentiation, hESC were split at a 1:5 ratio using 0.02% EDTA (Sigma-Aldrich, St. Louis, MO, USA) and mechanical scraping. After splitting, cells were cultured in StemPro medium for 24 h to let them attach to the plate. The next day (day 0), StemPro was replaced with N2B27 medium after gentle washing twice with Dulbecco's phosphate-buffered saline (DPBS; Life Technologies). N2B27 medium consists of DMEM/F12 (1:1) supplemented with 1 × N2 supplement, 1 × B27 supplement, 0.1 mmol/l β-mercaptoethanol, 1% non-essential amino acids solution (NEAA) and 0.5 mg/ml bovine serum albumin (all from Life Technologies). For trophoblast differentiation, four different conditions were used (**Figure 1A**): (i) BMP4, induction by 10 ng/ml BMP4 (PeproTech, NJ, USA) without inhibitors (marked in yellow throughout the study); (ii) 'iFGF2 + BMP4', induction by 10 ng/ml BMP4 and inhibition by 0.1 µmol/l fibroblast growth factor and vascular endothelial growth factor (FGF/VEGF) receptor tyrosine kinase inhibitor PD173074 (Santa Cruz Biotechnology, CA, USA) (marked in blue); (iii) 'iTGFb + BMP4', induction by 10 ng/ml BMP4 and inhibition by 1 µmol/l TGF-β type I receptors (ALK4/5/7) inhibitor A83–01 (Abcam, UK) (marked in green); and (iv) 'iFGF2 + iTGFb + BMP4', induction by 10 ng/ml BMP4 and co-inhibition by 0.1 µmol/l FGF/VEGF receptor inhibitor PD173074 and 1 µmol/l ALK4/5/7 inhibitor A83–01 (marked in red). Untreated hESC were marked in violet throughout the study. Media and supplements were replaced every 24 h. Every other day, for a period of 12 days (**Figure 1B**), two 35-mm plates of cells were dissociated in TRIzol

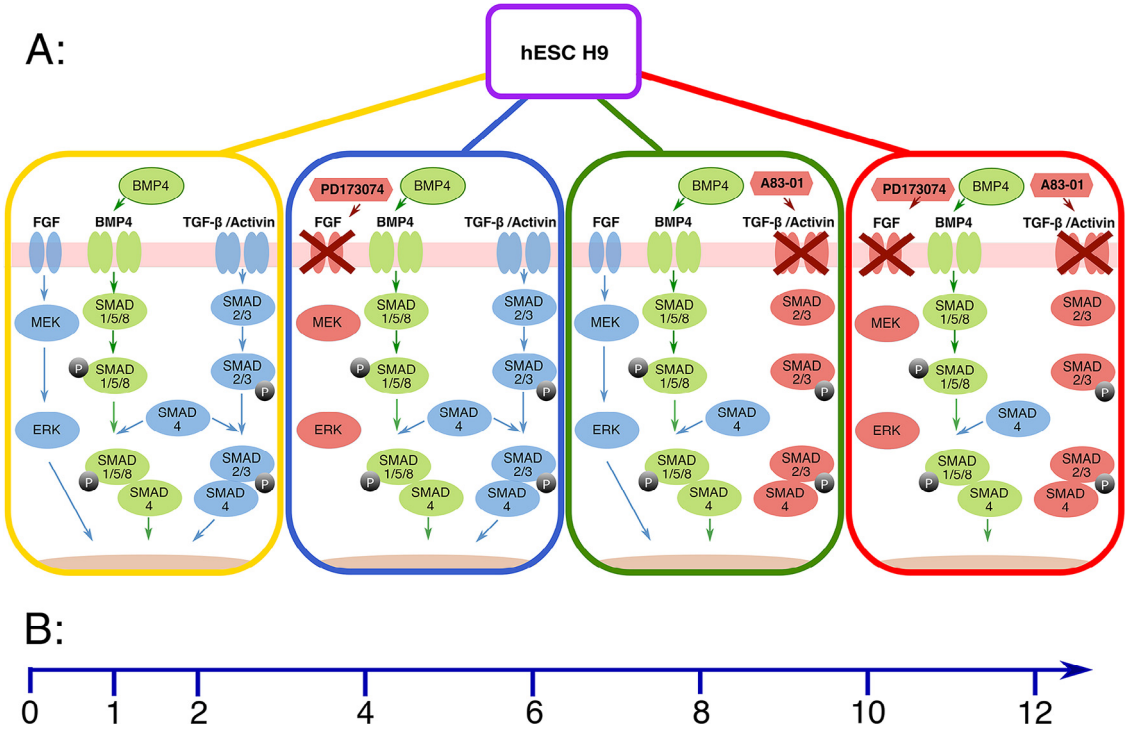

Figure 1 – Experimental design of hESC line H9 differentiation. The activated BMP4 pathway is shown in green and inhibited pathways and their inhibitors are shown in red. The unmanipulated pathways are in blue. (A) Coloured outlines of the figure represent the four conditions used: yellow, BMP4; blue, 'iFGF2 + BMP4'; green, 'iTGFb + BMP4' and red, 'iFGF2 + iTGFb + BMP4'. (B) Timeline of experimental design. Numbers show days when RNA samples were collected. Two replicas for every condition at every time point were used. BMP4 = bone morphogenic protein 4; FGF2 = fibroblast growth factor 2; hESC = human embryonic stem cells; TGF = transforming growth factor.

Reagent (Thermo Fisher Scientific), and cell culture medium was collected and stored at –80°C.

Placental samples

To assess the similarity of differentiating hESC and placental tissue on the transcriptomic level, full-thickness placental blocks of around 2–3 cm were taken from two full-term healthy pregnancies and stored at –80°C in RNAlater (Thermo Fisher Scientific, Waltham, MA, USA) within 1 h after normal delivery. Total placental RNA was extracted from frozen tissue with the mirVana™ miRNA Isolation Kit (Thermo Fisher Scientific) according to the manufacturer's instructions without isolation of small RNA. Extractions were performed from three samples collected from three locations of the same placenta, and all RNA samples from one placenta were pooled together. The study was approved by the Research Ethics Committee of the University of Tartu (permission no. 162/T-10) on 27 August 2007.

RNA isolation

The total RNA of treated cells was isolated using TRIzol Reagent following phenol/chloroform extraction and isopropanol precipitation. DNA contamination was removed from RNA samples with the DNA-free™ Kit (Thermo Fisher Scientific) according to the manufacturer's instructions. The Agilent 2100 Bioanalyser and RNA 6000 Nano Kit (Agilent Technologies, Santa Clara, CA, USA) were used to assess the RNA integrity number (RIN) and concentration of total RNA samples. All RIN values for differentiated hESC were >9 and >5.7 for placental samples. RNA concentrations were furthermore assessed by Qubit (Invitrogen) fluorometric quantitation. Altogether, 60 RNA samples (four conditions, seven time points, two replicates for every condition at every time point, plus two samples of undifferentiated hESC and two placental samples) were used for sample preparation for RNA sequencing.

Full transcriptome analysis using RNA sequencing (RNA-seq)

Bulk-RNA full transcriptome analysis of cultured hESC and placental tissue was performed by the RNA-seq method, following the single-cell tagged reverse transcription (STRT) protocol with modifications (Krjutškov et al., 2016). Ten nanogram of high-quality input RNA was converted to cDNA and amplified to form an Illumina-compatible library. In total, 25 PCR cycles were used, but as four base-pair unique molecular identifiers were applied, only the absolute number of unique reads was calculated per analysed sample. The libraries were sequenced by Illumina HiSeq2000, processed by Casava 1.8.2 (both Illumina, San Diego, CA, USA), and quality control was performed by STRTprep (https://github.com/shka/STRTprep, commit number 81a41adc7be5d388709b7f50504dc9a79ba72c25) (**Supplementary Table S1**).

The STRT computational analysis relies on two useful aspects. First, 5'-tagging of transcription start sites allows for promoter recognition in regulatory studies. Second, RNA-seq signal normalization based on synthetic spike-in RNA controls allows for unambiguous counting of input RNA contents instead of relative gene expression, as is commonly used, based on endogenous normalization.

Reads were aligned against the human hg19 genome and synthetic ERCC92 spike-in sequences using TopHat software ver. 2.0.10

(Kim et al., 2013). Reads aligning to spike-ins and 5' UTR regions were quantified by HTseq (ver. 0.6.1) (Anders et al., 2015). Spike-in-based normalization and differential expression analyses were performed with the R package edgeR (ver. 3.12.0) (Robinson and Oshlack, 2010), with false discovery rate (FDR) < 0.01 and fold change (FC) > 2 used as thresholds for differential expression. The involvement of genes on the KEGG pathways were predicted by GeneNetwork (http://genenetwork.nl/GeneNetwork/ (Fehrmann et al., 2015)) and the tissue-specific transcriptomes were mined using the Human Protein Atlas (Version: 14, http://www.proteinatlas.org). Figures were generated using R version 3.2.2 (R Core Team, 2015).

Validation by real-time PCR

cDNA was generated by following previously described efficient oligo-T priming (Krjutškov et al., 2016) by 1 µl of high-quality RNA sample at 10 ng/µl concentration. Real-time PCR was performed in triplicate using HOT FIREPol® EvaGreen® qRT-PCR Supermix (Solis BioDyne, Tartu, Estonia). Primer sequences are presented in **Supplementary Table S2**. Relative mRNA expression levels, compared with exogenous spike-in (pSPIKE1) (Thermo Fisher Scientific), were determined by the $\Delta\Delta C_T$ method.

The concordance between RNA-seq and quantitive reverse transcription-PCR (qRT-PCR) was analysed using an association test for Pearson correlation. Only samples for which expression values exceeded the detection limit in both compared methods were included in the analysis.

Measurement of secreted total and hyperglycosylated HCG

To analyse the secretion of trophoblast cells' specific hormone, differentiating hESC culture supernatants were collected, stored at –80°C, and the levels of total HCG and HCG-H were quantified by time-resolved immunofluorometric assay as described previously (Alfthan et al., 1992; Stenman et al., 2011).

Cytokeratin 7 immunostaining

To describe the pan-trophoblast marker protein cytokeratin 7 presence, cells differentiated until day 5 were fixed with ice-cold 100% methanol for 15 min at –20°C and washed three times with PBS. Fixed cells were incubated with UltraVision Protein Block (Thermo Fisher Scientific, LabVision Inc., Fremont, CA, USA) for 5 min, treated with primary antibody against cytokeratin 7 – KRT7 (Antibody Registry: AB_2265604, Santa Cruz Biotechnology, Inc., Dallas, TX, USA) and visualized with Alexa Fluor 488-conjugated donkey anti-mouse secondary antibody (Life Technologies, Eugene, OR, USA). The primary antibody was omitted in the negative control. For nuclear staining, cells were mounted with Vectashield mounting medium for fluorescence with DAPI (Vector Laboratories Inc., Burlingame, CA, USA). Stained cells were imaged using an EVOS FL Cell Imaging System (Thermo Fisher Scientific).

Results

Full transcriptome analysis using RNA sequencing

The progress of the hESC differentiation during the period of 12 days was assessed by RNA sequencing. Up- and down-regulated genes were identified for each time point, using hESC at day 0 as a reference (**Supplementary Figure S1** and **Supplementary Table S3**). The number of differentially expressed genes increased progressively during the course of differentiation under all conditions. However, there were fewer up-regulated genes after day 8 with the condition 'iTGFb + BMP4' when compared with the other inhibition conditions (**Supplementary Figure S1**). The number of down-regulated genes also increased similarly during the first days of differentiation. Next, the similarity between placental tissue and differentiated hESC was investigated. For that, genes up-regulated in placental tissue compared with hESC were identified and this list of genes was overlapped with the lists of genes up-regulated in the case of each condition and time point in differentiated hESC, compared with undifferentiated hESC. The number of overlapping genes was highest under the 'iFGF2 + BMP4' and 'iFGF2 + iTGFb + BMP4' conditions (**Figure 2**).

To compare the influence of different treatments on gene expression level, we performed the cluster analysis (**Figure 3**). Four clusters formed: (i) day 0, hESC samples; (ii) days 1 and 2, all conditions; (iii) days 4 and 6, all conditions, as well as days 8 and 12 with the 'iTGFb + BMP4' condition; and (iv) day 8 and beyond, all conditions, except the 'iTGFb + BMP4' condition. The fact that the transcriptome profile for days 8–12 for TGF-β/activin/nodal inhibition with BMP4 activation corresponded to the profiles for days 4–6 for the rest of the conditions suggest an overall deceleration of BMP4-mediated hESC differentiation in the presence of TGF-β/activin/nodal inhibition.

Cell type-specific marker gene detection

To analyse the direction of hESC differentiation, the expression of known cell type marker genes was investigated. Full transcriptome analysis revealed no detectable expression of genes specific for primitive streak (*T* and *MIXL1*), mesoderm (*GSC*, *CD34*, *TWIST1* and *FOXF1*), endoderm (*SOX7*, *GATA4*, *GATA6*, *SOX17*, *FOXA2* and *AFP*) and ectoderm (*SOX1*, *NES* and *NCAM*) at any conditions and any time points. As expected, several hESC-specific genes such as *POU5F1*, *POLR3G*, *NANOG*, *DPPA4* and *MYC* were down-regulated (**Supplementary Table S3**). To investigate the hESC differentiation to trophoblast-like cells the known markers from a previous study (Lee et al., 2016) were investigated at all time points and conditions. Trophoblast-like cell formation was supported with all conditions apart from 'iTGFb + BMP4', as samples treated by 'BMP4' from day 6 and by 'iFGF2 + BMP4' and 'iFGF2 + iTGFb + BMP4' from day 8 and beyond clustered together and had higher expression of syncytiotrophoblast-specific markers (**Supplementary Figure S2**).

Validation of the RNA sequencing results

To check the accuracy of the RNA sequencing results, some of the significantly regulated cell type marker genes (*CGB5*, *CYP11A1*, *DUSP6*, *GATA3*, *MMP9*, *POU5F1*, *TGFBI*, *TIMP1*) were validated using qRT-PCR at all conditions at every time point (**Supplementary Figure S3**), and showing the concordance between the two methods. The expression of some known marker genes that were undetectable by RNA sequencing was examined by immunofluorescence (IF) in the case of *KRT7* or qRT-PCR for *GCM1*, *HLA-G*, *KRT7*, *NCAM*, *SOX17* and *T*. For example, on day 5, pan-trophoblast marker cytokeratin 7 (KRT7) was detected at the protein level by IF in most of the cells with 'iFGF2 + BMP4' and BMP4 alone, but only in a few cells with 'iFGF2 + iTGFb + BMP4' and 'iTGFb + BMP4' conditions (**Supplementary Figure S4**). This discrepancy between IF and RNA-seq results may be caused by the low

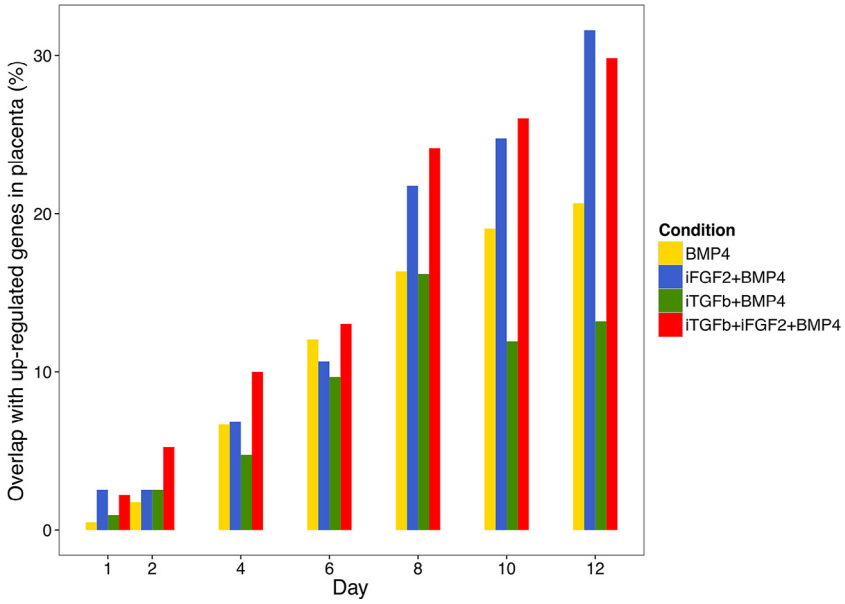

Figure 2 – Overlap between differentially expressed genes and placenta-specific genes during the 12 days of hESC differentiation. Differentially expressed genes were identified in comparison with undifferentiated hESC on day 0. hESC = human embryonic stem cells.

expression level of the *KRT7* gene, confirmed by qRT-PCR. The syncytiotrophoblast marker *GCM1* was up-regulated on days 8, 10 and 12 after the start of FGF2 inhibition together with BMP4 activation, while the EVT marker *HLA-G*, on the other hand, was undetectable in most of the samples as revealed by qRT-PCR (**Supplementary Figure S5**). The expression of early endoderm marker brachyury (*T*) was up-regulated with all conditions, however the expression was relatively low. There was no expression of early ectoderm marker *SOX17*, but the ectoderm marker *NCAM* was detected under all conditions of differentiation (**Supplementary Figure S5**). The RNA-seq expression levels of several most differentially expressed genes (*CALB1*, *THY1*, *CRYAB*, *EMX2*, *BNIPL* and *MMP9*) were validated by qRT-PCR. Despite the fact that the expression was usually below the detection limit for one of the conditions, making the fold changes from two different methods directly incomparable, the direction of expression change for all tested genes demonstrated the validity of the results of differential expression analysis methods (**Figure 4**). The presence of endogenous FGF2 and activin A expression was also confirmed on the mRNA level by qRT-PCR during the differentiation protocol (**Supplementary Figure S6**).

Measurements of HCG

Secretion of the trophoblast hormone HCG was measured from cell culture supernatants throughout differentiation. HCG-H was secreted from day 8 onwards in the case of FGF2 inhibition with BMP4 activation, or in combination with inhibition by the FGF2 and TGF-β/activin/nodal pathway with BMP4 activation. The secretion of HCG and its hyperglycosylated form HCG-H was highest on day 12 in the case of treatment with BMP4 and inhibition of FGF2 (**Figure 5**), showing that FGF2 inhibition is essential for HCG-producing trophoblast-like cells forming.

The effect of FGF2 inhibition on BMP4-mediated trophoblast differentiation

To investigate the role of FGF2 inhibition in trophoblast formation, the samples treated with FGF2 inhibitor together with BMP4 activator were compared with control samples treated with BMP4 only. The differences in gene expression appeared at the last two time points (days 10 and 12) when 45 and 42 genes were significantly up- and down-regulated (**Supplementary Table S4**).

The Human Protein Atlas was used to investigate which tissues express the largest number of up-regulated genes after FGF2 inhibition and BMP4 activation. The highest number of 'iFGF2 + BMP4' induced genes (42 out of 45 genes) were found to be present in the placental transcriptome (**Supplementary Figure S7A**), and among those, *LGALS16* and *CGB5* were unique to placenta. Only three genes expressed in hESC-derived trophoblasts were not shown to be expressed in placenta (*BHMT*, *CALB1* and *RIMS2*). However, *CALB1* probably associated with human developing trophoblasts (Belkacemi et al., 2003), being therefore relevant for undifferentiated trophoblasts and not for fully formed placenta.

To understand whether the added inhibitors could assist any relevant biological effect, the pathways associated with up- and down-regulated genes in the case of FGF2 inhibition and BMP4 activation were predicted (**Figure 6**). The largest numbers of up-regulated genes were involved in pathways associated with cellular focal adhesion, extracellular matrix (ECM)–receptor interactions, regulation of the actin cytoskeleton, and tight junctions. In addition, the genes related to the leukocyte transendothelial migration pathway were also up-regulated (e.g. *HOPX*, *PDGFRB*, *CRYAB*, *TPM1* and *ITGB1*). On the contrary, the genes related to pyrimidine and purine metabolism, DNA replication, base excision repair, nucleotide excision repair, mismatch repair, homologous recombination and cell cycle regulation were significantly down-regulated (**Figure 6**).

The effect of TGF-β/activin/nodal inhibition to the BMP4-mediated trophoblast differentiation

On days 10 and 12, TGF-β/activin/nodal inhibition with BMP4 activation led to a global down-regulation of gene expression when compared with the control condition (**Supplementary Table S4**). The number of down-regulated genes (n = 127) was approximately three times higher,

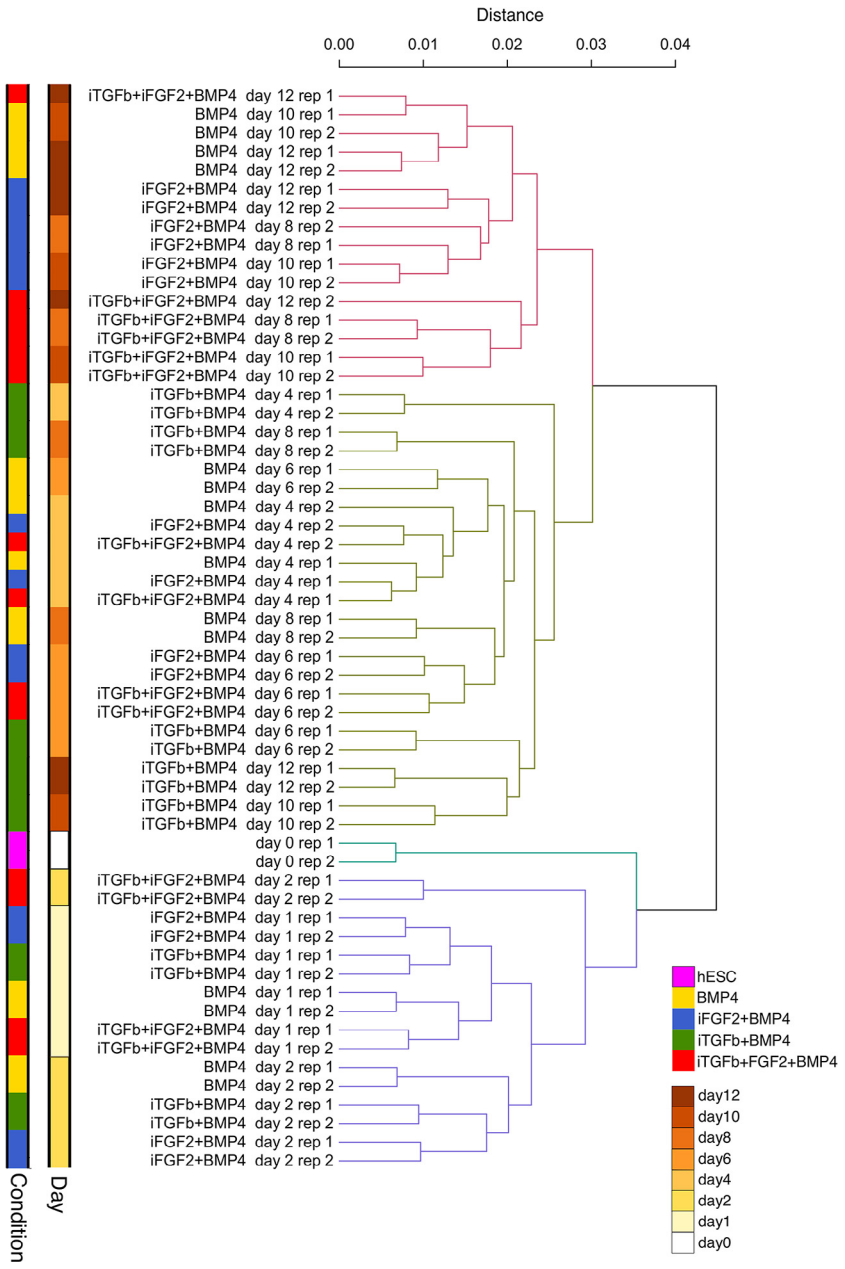

Figure 3 – Unsupervised hierarchical clustering of gene expression. Clustering of the samples is based on Pearson correlation and average linkage. Four formed clusters are marked with different colours: blue, day 0, hESC samples; violet, days 1 and 2, all conditions; green, days 4 and 6, all conditions, as well as days 8 and 12 with the 'iTGFb + BMP4' condition; red, day 8 and beyond, all conditions, except the 'iTGFb + BMP4' condition. BMP4 = bone morphogenic protein 4; hESC = human embryonic stem cells; TGF = transforming growth factor.

and the number of up-regulated genes ($n = 5$) was 9 to 12 times lower when compared with the other conditions. The pathways connected with down-regulated genes during TGF-β/activin/nodal inhibition and BMP4 activation were analogous to those associated with genes up-regulated during FGF2 inhibition combined with BMP4 activation (**Supplementary Figure S8a**). For example, 'iTGFb + BMP4' caused down-regulation of pathways related to focal adhesion, extracellular matrix–receptor interactions and leukocyte transendothelial migration. Therefore, FGF2 and TGF-β/activin/nodal inhibition have rather opposite effects in the cells differentiated by BMP4. The combination of the two inhibitors ('iFGF2 + iTGFb + BMP4' condition) led to the regulation of pathways identified under both inhibitory conditions separately, indicating that the effect of two added inhibitors is probably not combined (**Supplementary Figure S8b**).

TGF-β/activin/nodal inhibition with BMP4 activation decreased the ability of cells to achieve an invasive phenotype by down-regulating several cancer-related pathways and EVT marker genes (*MMP2*, *MMP9*, *SERPINE1* and *FN1*) after 10–12 days of treatment (**Supplementary Table S4**). Most of the down-regulated genes were also found to be expressed in placenta according to the Human Protein Atlas database (data not shown), indicating that the inhibition of TGF-β with BMP4 activation does not support the differentiation of hESC

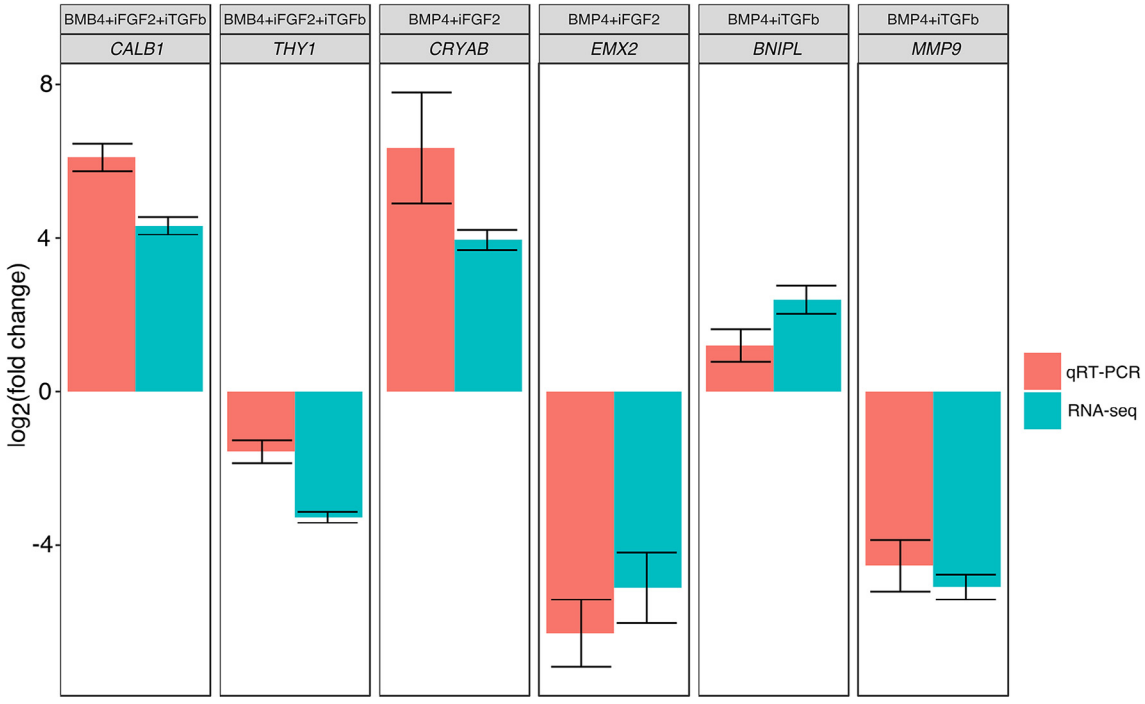

Figure 4 – qRT-PCR and RNA-seq analysis of the most differentially expressed genes between the inhibitions together with BMP4 activation, when compared with BMP4 activation alone measured on days 10 and 12 (two replicates per day). The figure presents the combined data for the two days. On the y-axis is the $\log_2$(fold change). qRT-PCR value was calculated: $\log_2(2^{-[\Delta Ct \text{ gene of interest} - \Delta Ct \text{ gene of interest with BMP4}]})$ and RNA-seq value was calculated: $\log_2$(ΔCt gene of interest) – $\log_2$(ΔCt gene of interest with BMP4). ΔCt = Ct (gene of interest) – Ct (pSPIKE1). The normalized read count of RNA-seq lower than one is equalized with one read. qRT-PCR is marked with red and RNA-seq is marked with blue. Error bars show the standard error of the mean (SEM). BMP4 = bone morphogenic protein 4; qRT-PCR = quantitive reverse transcription-PCR; RNA-seq = RNA-sequencing. (For interpretation of the references to colour in this figure legend, the reader is referred to the web version of this article.)

toward trophoblast-like cells. Notably, several known members of the TGF-β signalling pathway were also down-regulated (e.g. *DCN*, *DIO3*, *GANAB* and *TGFBI*), demonstrating the effect of TGF-β/activin/nodal inhibition (**Supplementary Table S4**).

When the up-regulated genes following the 'iTGFb + BMP4' (n = 5) and 'iTGFb + iFGF2 + BMP4' (n = 61) conditions (**Supplementary Table S4**) were compared with the tissues available at the Human Protein Atlas database, a lower similarity with the placental transcriptome was seen (**Supplementary Figure S7B** and **C**, respectively), when compared with the FGF2-induced trophoblast-like cells (**Supplementary Figure S7A**).

Discussion

Since the first report in 2002, BMP4 induction with or without TGF-β/activin/nodal and FGF2 inhibition has been used to differentiate trophoblast cells from hESC (Amita et al., 2013; Chen et al., 2013; Das et al., 2007; Erb et al., 2011; Lee et al., 2015; Li et al., 2013, p. 4; Marchand et al., 2011; Sudheer et al., 2012; Telugu et al., 2013; Xu et al., 2002; Yang et al., 2015). Although several research groups have been working with this model to improve the differentiation effectiveness and to obtain as pure trophoblast populations as possible, most of the studies have not investigated systematically how much these inhibitors improve the differentiation of cells compared with the basic BMP4 treatment and which are the separate effects of TGF-β/activin/nodal and FGF2 pathways. One of the landmark studies in this field was conducted by Sudheer et al. (2012), who pointed out that FGF2 inhibition forces syncytiotrophoblast formation from hESC. However, in 2011 Bernardo et al. (2011) expressed doubts about whether this method can support the formation of trophoblasts from hESC (Bernardo et al., 2011; Roberts et al., 2014), opening up the still unsolved debate about the importance of TGF-β and FGF2 pathway inhibition in BMP4-triggered trophoblast differentiation. Therefore, this current study aimed to investigate how the inhibitors of the TGF-β/activin/nodal and FGF2 signalling pathways change the gene expression of cells during the BMP4-mediated hESC differentiation into trophoblast-like cells.

This study investigated comprehensively the molecular effects of both inhibitors during the first 12 days of hESC treatment with BMP4, in order to understand how much the inhibitors can improve the efficiency of hESC differentiation when compared with the basic BMP4 treatment. For this purpose, gene expression profiling by RNA sequencing was performed. Surprisingly, the effects of the inhibitors were not apparent during the first 6–8 days of the differentiation, as no significantly differentially expressed genes were detected when compared with BMP4 induction only and all conditions were similar when the gene expression pattern at each time point and treatment condition was compared with that of hESC (**Supplementary Figure S1**) or placental tissue (**Figure 2**). However, starting from day 8, the number of up-regulated genes and the similarity with placental tissue increased faster when, in addition to BMP4 activator, FGF2 inhibitor

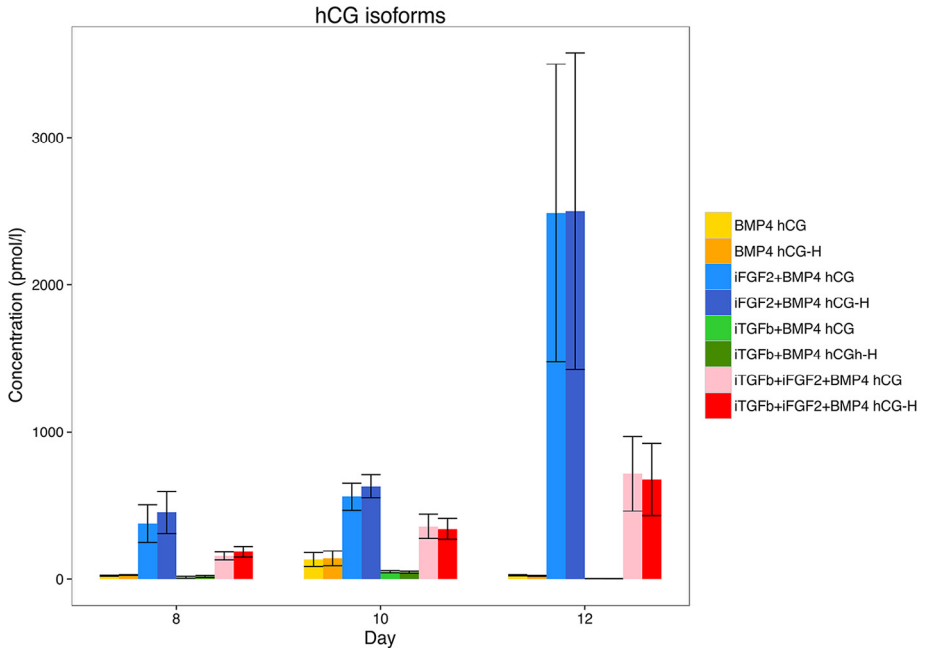

Figure 5 – ELISA measurement of the concentration of total HCG and hyperglycosylated HCG (HCG-H) in the cells' growth media. Different treatment groups are shown with different colours and error bars show the minimum and maximum value of the two replicates. HCG = human chorionic gonadotrophin.

was used alone or in combination with TGF-β/activin/nodal inhibition. In contrast, the inhibition of the TGF-β/activin/nodal pathway together with BMP4 activation seemed to change the rate of differentiation from day 6 onward more slowly (**Supplementary Figure S1**). The reason for the absence of the effects of the inhibitors before day 8 of the differentiation might be the lack of activin A in our cell culture media before 8 days of differentiation.

The general suppressive effect of TGF-β/activin/nodal inhibition became evident when the gene expression profiles were compared with that of sole BMP4 induction. The lowest number of up-regulated genes (n = 5) and the highest number of down-regulated genes (n = 127) were detected for TGF-β/activin/nodal inhibition with BMP4 activation. The cluster analysis confirmed that during TGF-β/activin/nodal inhibition, total transcriptional activity lags behind, compared with other induction and inhibition conditions. This was evident, because the transcriptome profile for days 8–12 for TGF-β/activin/nodal inhibition with BMP4 activation corresponded to the profiles for days 4–6 for the rest of the conditions. The same trend was observed when different conditions were clustered based on the expression of trophoblast-specific marker genes known from the previous publication (Lee et al., 2016). Although several extravillous trophoblast-specific transcripts were not detectable (e.g. *HLA-G*, *CDH5*, *ITGA1* and *ASCL2*), it is still notable that from day 8 onwards, all the other conditions except for TGF-β/activin/nodal inhibition with BMP4 activation were clustered together based on the higher expression of syncytiotrophoblast marker genes like *CGB5*, *CGA*, *MMP2* and *MMP9*. This phenomenon suggests that, during the first days of differentiation, BMP4 treatment alone was crucial for cellular differentiation, while TGF-β/activin/nodal inhibition delayed further differentiation of hESC into trophoblast-like cells.

The immunostaining of pan-trophoblast marker KRT7 confirmed that the 'iFGF2 + BMP4' condition guided the differentiation of most of the cells toward trophoblast-like cells. Although several embryonic cell fate markers were not detected by sequencing (*MIXL1*, *GSC*, *FOXF1*, *SOX7*, *GATA4*, *GATA6*, *SOX17*, *FOXA2*, *SOX1* and *NES*), RT-qPCR showed low expression and slight up-regulation of primitive streak and ectoderm markers (*T* and *NCAM*, respectively). However, *NCAM* has also been related to the differentiation of trophoblast cells (Blankenship and King, 1996). Similarly to Yabe et al. (2016), *HLA-G* was not detected in most of the conditions, showing the method's inability to guide the formation of EVT cells.

A number of genes up-regulated by FGF2 inhibition compared with BMP4 treatment alone have been detected in placenta and are relevant for the formation of the trophoblast's phenotype. At the top of this list are placental-specific genes such as *CGB5*, *CGA*, *CYP11A1* and *LGALS16* that are also marker genes for syncytiotrophoblasts, confirming the results of Sudheer et al. (2012) and Yang et al. (2015), who proposed that FGF2 inhibition is essential for the formation of HCG-producing syncytiotrophoblasts. Interestingly, when the FGF2 inhibition was combined with the TGF-β/activin/nodal inhibition and complemented with BMP4 activator, the number of up-regulated genes that are also expressed in placenta dropped (**Supplementary Figure S7C**) and many of the trophoblast-specific genes were not differentially expressed compared with BMP4 treatment alone. Therefore, our transcriptomic-based results emphasize that sole FGF2 inhibition with BMP4 activation is sufficient to improve the syncytiotrophoblast formation.

To identify pathways activated in response to TGF-β/activin/nodal and FGF2 inhibition during trophoblastic differentiation mediated by BMP4 activation, we predicted the common functions for up- and down-regulated genes. For BMP4 activation with sole FGF2 or TGF-β/activin/nodal and FGF2 co-inhibition, several up-regulated genes were related to cell-to-cell interactions, to extracellular matrix adhesion, and to leukocyte transendothelial migration. As the key players participating in these processes are very similar to those regulating the trophoblasts' biology in embryo implantation, these results suggest

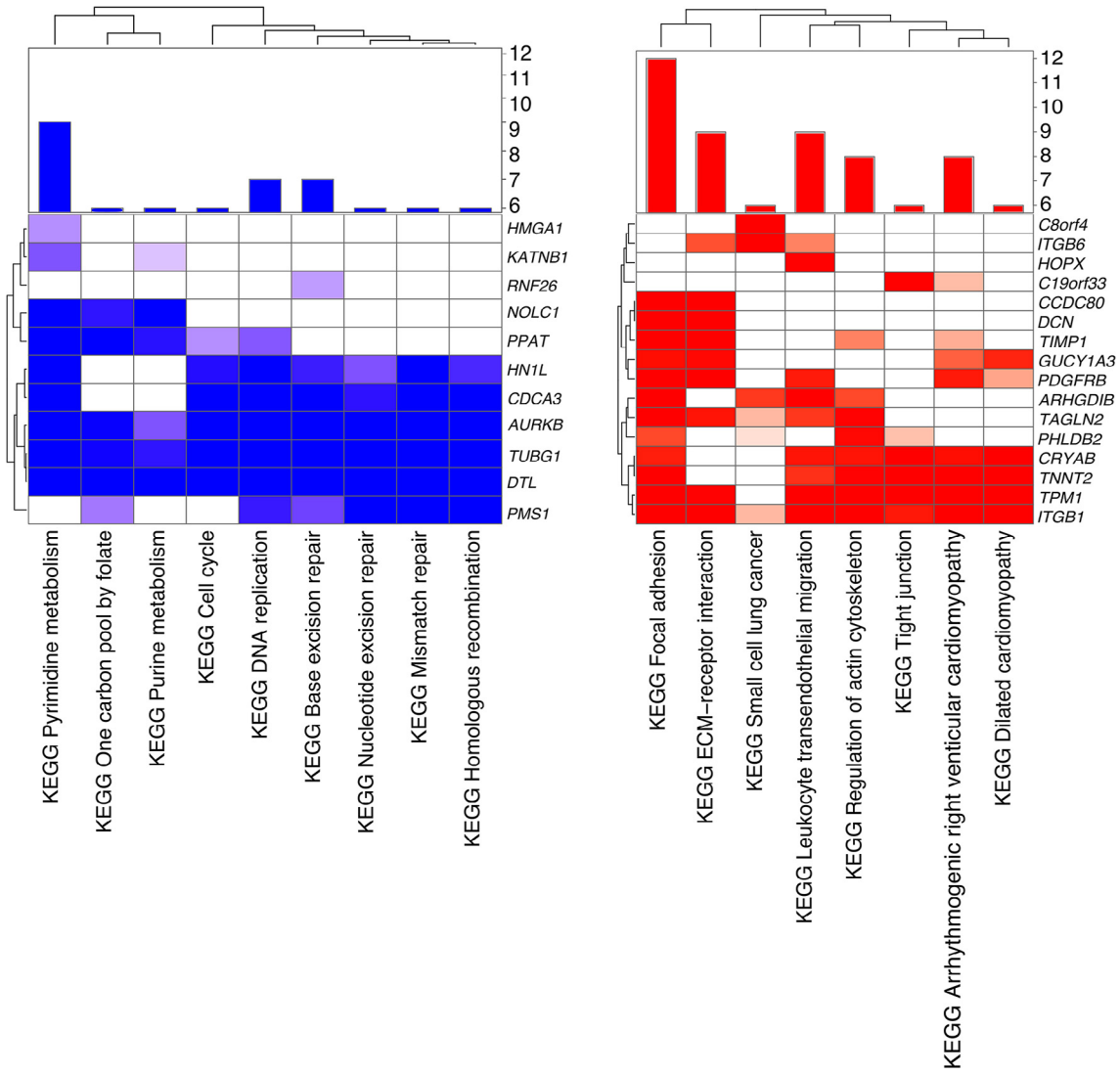

Figure 6 – Co-regulation-based functional enrichment of significantly up- and down-regulated genes of differentiated hESC with FGF2 inhibition and BMP4 activation. On the heat map, the significant pathways from the co-regulation-based functional prediction tool GeneNetwork are visualized. Only pathways with at least six involved genes are visualized. The darker colour indicates a lower *P*-value, while white cells indicate a *P*-value of >0.05. Clustering of the heat map is based on Euclidean distance and complete linkage. The number of genes predicted for involvement in each pathway is shown on the bar plots. Blue (left) depicts down-regulated genes and red (right) indicates upregulated genes. FGF2 = fibroblast growth factor 2; hESC = human embryonic stem cells. (For interpretation of the references to colour in this figure legend, the reader is referred to the web version of this article.)

that FGF2 inhibition with BMP4 activation supports trophoblastic differentiation. Moreover, results from this study indicate that FGF2 inhibition is more dominant in the 'iFGF2 + iTGFb + BMP4' condition because almost all up-regulated pathways in the case of 'iFGF2 + BMP4' were also present in the case with both inhibitors, with FGF2 inhibition probably rescuing the defects associated with TGF-β inhibition.

It was shown for the first time that BMP4 activation with FGF2 inhibition down-regulated several genes associated with the cell cycle, DNA replication, and pyrimidine/purine metabolism. This suggests that cell cycle arrest and cellular senescence, occurring during syncytiotrophoblast formation (Chuprin et al., 2013), is regulated by FGF2 inhibition. However, the higher expression of syncytiotrophoblast marker genes in the condition with 'iFGF2 + BMP4' rather than with 'iFGF2 + iTGFb + BMP4' may indicate a possible role for TGF-β/activin/nodal activation in trophoblast differentiation. Indeed, it has been shown that the loss of activin/nodal inhibition leads to the formation of syncytiotrophoblast cells (Sarkar et al., 2015), which also explains why we demonstrated fewer syncytiotrophoblast marker genes following double inhibition. In experiments from this study, used media did not contain ligands for the TGF-β/activin/nodal pathway. However, we detected the endogenous expression of INHBA, encoding a member of the TGF-β superfamily of proteins, in all used conditions from day 6 onwards (**Supplementary Figure S6**). Thus, in conditions with BMP4 activation and FGF2 pathway inhibition only, endogenous TGF-β superfamily proteins could be present and may favour the differentiation of syncytiotrophoblasts. In addition, the TGF-β activation pathway involves SMAD4 transcription factor, which is also included in the BMP4 pathway. Although these two pathways share common modulators, it is unlikely that endogenous TGF-β activation could entirely replace

BMP4 activation in trophoblast differentiation. Still, the exact consequences of TGF-β activation and inhibition remain speculative and need to be studied by future experiments.

This study demonstrated that the inhibition of FGF2 together with BMP4 activation resulted in predominant secretion of the hyperglycosylated isoform of HCG (HCG-H), which has been shown to be secreted by EVT cells, cytotrophoblast cells or stem trophoblast cells (Cole, 2007). Thus, we propose that secretion of HCG-H is merely a sign of yet incomplete differentiation of cytotrophoblast cells. This may be the reason why the late syncytiotrophoblast fusion marker GCM1 was expressed at a very low level, starting from day 8 of differentiation.

TGF-β/activin/nodal inhibition has been suggested to have a more central role in the generation of EVT cells (Sarkar et al., 2015). However, results from this study indicate that TGF-β/activin/nodal inhibition mainly causes gene expression down-regulation, when added to the BMP4 treatment. For example, EVT marker genes (*MMP2*, *MMP9*, *SERPINE1* and *FN1*) were significantly down-regulated after 10–12 days of treatment. Discrepancies between the current and previous studies may be caused by differences in experimental conditions (like cell culture media used) and analyses carried out, indicating the need for more comprehensive multi-omics analyses.

In summary, we observed that the effects of FGF2 and TGF-β/activin/nodal pathway inhibitors were undetectable before day 8 of differentiation, with BMP4 activation and FGF2 inhibition guiding hESC differentiation toward syncytiotrophoblasts, causing cellular senescence and fusion by down-regulating cell cycle genes and up-regulating the production of hyperglycosylated HCG. In contrast, BMP4 activation complemented with TGF-β/activin/nodal inhibition decreased the ability of hESC to differentiate toward trophoblastic lineages and was therefore found to be a suboptimal strategy for these purposes. Consequently, these findings clearly show that BMP4 activation in combination with FGF2 inhibition is the most suitable protocol for hESC differentiation toward trophoblast-like cells and additional inhibition of TGF-β/activin/nodal is not necessary.

Acknowledgements

This work was supported by the EU FP7-PEOPLE-2012-IAPP grant SARM (grant no. 324509), by the Estonian Ministry of Education and Research (grant IUT34-16), the EU-FP7 Eurostars Programme (grant NOTED, EU41564), Enterprise Estonia (grants EU30020 and EU48695), H2020-TWINN-2015 Project WIDENLIFE (grant no. 692056), Karolinska Institute Distinguished Professor Award to Prof. Juha Kere, the Swedish Research Council, and the Strategic Research Programme for Diabetes funding at the Karolinska Institute. Part of this work was assisted by the Karolinska High Throughput Centre, a core facility at the Karolinska Institute affiliated with SciLifeLab (https://www.scilifelab.se/facilities/khtc/). Computations were performed on resources provided by the Swedish National Infrastructure for Computing (SNIC) via the Uppsala Multidisciplinary Centre for Advanced Computational Science (UPPMAX) under Project b2014069. The language of the manuscript was corrected by Oxford Language Editing.

Appendix: Supplementary material

Supplementary data to this article can be found online at doi:10.1016/j.rbmo.2017.06.003.

ARTICLE INFO

Article history:
Received 29 November 2016
Received in revised form 19 May 2017
Accepted 1 June 2017
Declaration: The authors report no financial or commercial conflicts of interest.

Keywords:
bone morphogenic protein 4
fibroblast growth factor 2
human embryonic stem cell
placenta
transforming growth factor-β
trophoblast cells

REFERENCES

Alfthan, H., Haglund, C., Dabek, J., Stenman, U.H., 1992. Concentrations of human choriogonadotrophin, its beta-subunit, and the core fragment of the beta-subunit in serum and urine of men and nonpregnant women. Clin. Chem. 38, 1981–1987.

Amita, M., Adachi, K., Alexenko, A.P., Sinha, S., Schust, D.J., Schulz, L.C., Roberts, R.M., Ezashi, T., 2013. Complete and unidirectional conversion of human embryonic stem cells to trophoblast by BMP4. Proc. Natl. Acad. Sci. U.S.A. 110, E1212–E1221. doi:10.1073/pnas.1303094110.

Anders, S., Pyl, P.T., Huber, W., 2015. HTSeq – a Python framework to work with high-throughput sequencing data. Bioinformatics 31, 166–169. doi:10.1093/bioinformatics/btu638.

Belkacemi, L., Gariépy, G., Mounier, C., Simoneau, L., Lafond, J., 2003. Expression of calbindin-D28k (CaBP28k) in trophoblasts from human term placenta. Biol. Reprod. 68, 1943–1950. doi:10.1095/biolreprod.102.009373.

Bernardo, A.S., Faial, T., Gardner, L., Niakan, K.K., Ortmann, D., Senner, C.E., Callery, E.M., Trotter, M.W., Hemberger, M., Smith, J.C., Bardwell, L., Moffett, A., Pedersen, R.A., 2011. BRACHYURY and CDX2 mediate BMP-induced differentiation of human and mouse pluripotent stem cells into embryonic and extraembryonic lineages. Cell Stem Cell 9, 144–155. doi:10.1016/j.stem.2011.06.015.

Blankenship, T.N., King, B.F., 1996. Macaque intra-arterial trophoblast and extravillous trophoblast of the cell columns and cytotrophoblastic shell express neural cell adhesion molecule (NCAM). Anat. Rec. 245, 525–531. doi:10.1002/(SICI)1097-0185(199607)245:3<525::AID-AR9>3.0.CO;2-Q.

Chen, Y., Wang, K., Chandramouli, G.V.R., Knott, J.G., Leach, R., 2013. Trophoblast lineage cells derived from human induced pluripotent stem cells. Biochem. Biophys. Res. Commun. 436, 677–684. http://dx.doi.org/10.1016/j.bbrc.2013.06.016.

Chuprin, A., Gal, H., Biron-Shental, T., Biran, A., Amiel, A., Rozenblatt, S., Krizhanovsky, V., 2013. Cell fusion induced by ERVWE1 or measles virus causes cellular senescence. Genes Dev. 27, 2356–2366. doi:10.1101/gad.227512.113.

Cole, L.A., 2007. Hyperglycosylated hCG. Placenta 28, 977–986. doi:10.1016/j.placenta.2007.01.011.

Das, P., Ezashi, T., Schulz, L.C., Westfall, S.D., Livingston, K.A., Roberts, R.M., 2007. Effects of FGF2 and oxygen in the BMP4-driven differentiation of trophoblast from human embryonic stem cells. Stem Cell Res. 1, 61–74. doi:10.1016/j.scr.2007.09.004.

Erb, T.M., Schneider, C., Mucko, S.E., Sanfilippo, J.S., Lowry, N.C., Desai, M.N., Mangoubi, R.S., Leuba, S.H., Sammak, P.J., 2011. Paracrine and epigenetic control of trophectoderm differentiation

from human embryonic stem cells: the role of bone morphogenic protein 4 and histone deacetylases. Stem Cells Dev. 20, 1601–1614. doi:10.1089/scd.2010.0281.

Fehrmann, R.S.N., Karjalainen, J.M., Krajewska, M., Westra, H.-J., Maloney, D., Simeonov, A., Pers, T.H., Hirschhorn, J.N., Jansen, R.C., Schultes, E.A., van Haagen, H.H.H.B.M., de Vries, E.G.E., te Meerman, G.J., Wijmenga, C., van Vugt, M.A.T.M., Franke, L., 2015. Gene expression analysis identifies global gene dosage sensitivity in cancer. Nat. Genet. 47, 115–125. doi:10.1038/ng.3173.

Kim, D., Pertea, G., Trapnell, C., Pimentel, H., Kelley, R., Salzberg, S.L., 2013. TopHat2: accurate alignment of transcriptomes in the presence of insertions, deletions and gene fusions. Genome Biol. 14, R36. doi:10.1186/gb-2013-14-4-r36.

Krjutškov, K., Katayama, S., Saare, M., Vera-Rodriguez, M., Lubenets, D., Samuel, K., Laisk-Podar, T., Teder, H., Einarsdottir, E., Salumets, A., Kere, J., 2016. Single-cell transcriptome analysis of endometrial tissue. Hum. Reprod. 31, 844–853. doi:10.1093/humrep/dew008.

Lee, C.Q.E., Gardner, L., Turco, M., Zhao, N., Murray, M.J., Coleman, N., Rossant, J., Hemberger, M., Moffett, A., 2016. What is trophoblast? A combination of criteria define human first-trimester trophoblast. Stem Cell Reports 6, 257–272. doi:10.1016/j.stemcr.2016.01.006.

Lee, Y.-L., Fong, S.-W., Chen, A.C.H., Li, T., Yue, C., Lee, C.-L., Ng, E.H.Y., Yeung, W.S.B., Lee, K.-F., 2015. Establishment of a novel human embryonic stem cell-derived trophoblastic spheroid implantation model. Hum. Reprod. 30, 2614–2626. doi:10.1093/humrep/dev223.

Li, Y., Moretto-Zita, M., Soncin, F., Wakeland, A., Wolfe, L., Leon-Garcia, S., Pandian, R., Pizzo, D., Cui, L., Nazor, K., Loring, J.F., Crum, C.P., Laurent, L.C., Parast, M.M., 2013. BMP4-directed trophoblast differentiation of human embryonic stem cells is mediated through a ΔNp63+ cytotrophoblast stem cell state. Development 140, 3965–3976. doi:10.1242/dev.092155.

Lichtner, B., Knaus, P., Lehrach, H., Adjaye, J., 2013. BMP10 as a potent inducer of trophoblast differentiation in human embryonic and induced pluripotent stem cells. Biomaterials 34, 9789–9802. http://dx.doi.org/10.1016/j.biomaterials.2013.08.084.

Marchand, M., Horcajadas, J.A., Esteban, F.J., McElroy, S.L., Fisher, S.J., Giudice, L.C., 2011. Transcriptomic signature of trophoblast differentiation in a human embryonic stem cell model. Biol. Reprod. 84, 1258–1271. doi:10.1095/biolreprod.110.086413.

R Core Team, 2015. R: A Language and Environment for Statistical Computing. R Foundation for Statistical Computing, Vienna, Austria. https://www.R-project.org/.

Roberts, R.M., Loh, K.M., Amita, M., Bernardo, A.S., Adachi, K., Alexenko, A.P., Schust, D.J., Schulz, L.C., Telugu, B.P.V.L., Ezashi, T., Pedersen, R.A., 2014. Differentiation of trophoblast cells from human embryonic stem cells: to be or not to be? Reproduction 147, D1–D12. doi:10.1530/REP-14-0080.

Robinson, M.D., Oshlack, A., 2010. A scaling normalization method for differential expression analysis of RNA-seq data. Genome Biol. 11, R25. doi:10.1186/gb-2010-11-3-r25.

Sarkar, P., Randall, S.M., Collier, T.S., Nero, A., Russell, T.A., Muddiman, D.C., Rao, B.M., 2015. Activin/Nodal signaling switches the terminal fate of human embryonic stem cell-derived trophoblasts. J. Biol. Chem. 290, 8834–8848. doi:10.1074/jbc.M114.620641.

Shirley, M.L., Venable, A., Rao, R.R., Boyd, N.L., Stice, S.L., Puett, D., Narayan, P., 2012. Bone morphogenetic protein-4 affects both trophoblast and non-trophoblast lineage-associated gene expression in human embryonic stem cells. Stem Cell Discov. 2, 163–175. doi:10.4236/scd.2012.24021.

Stenman, U.-H., Birken, S., Lempiäinen, A., Hotakainen, K., Alfthan, H., 2011. Elimination of complement interference in immunoassay of hyperglycosylated human chorionic gonadotrophin. Clin. Chem. 57, 1075–1077. doi:10.1373/clinchem.2010.159939.

Sudheer, S., Bhushan, R., Fauler, B., Lehrach, H., Adjaye, J., 2012. FGF inhibition directs BMP4-mediated differentiation of human embryonic stem cells to syncytiotrophoblast. Stem Cells Dev. 21, 2987–3000. doi:10.1089/scd.2012.0099.

Telugu, B.P., Adachi, K., Schlitt, J.M., Ezashi, T., Schust, D.J., Roberts, R.M., Schulz, L.C., 2013. Comparison of extravillous trophoblast cells derived from human embryonic stem cells and from first trimester human placentas. Placenta 34, 536–543. http://dx.doi.org/10.1016/j.placenta.2013.03.016.

Teo, A.K.K., Ali, Y., Wong, K.Y., Chipperfield, H., Sadasivam, A., Poobalan, Y., Tan, E.K., Wang, S.T., Abraham, S., Tsuneyoshi, N., Stanton, L.W., Dunn, N.R., 2012. Activin and BMP4 synergistically promote formation of definitive endoderm in human embryonic stem cells. Stem Cells 30, 631–642. doi:10.1002/stem.1022.

Vallier, L., Alexander, M., Pedersen, R.A., 2005. Activin/Nodal and FGF pathways co-operate to maintain pluripotency of human embryonic stem cells. J. Cell Sci. 118, 4495–4509. doi:10.1242/jcs.02553.

Xu, R., Chen, X., Li, D.S., Li, R., Addicks, G.C., Glennon, C., Zwaka, T.P., Thomson, J.A., 2002. BMP4 initiates human embryonic stem cell differentiation to trophoblast. Nat. Biotechnol. 20, 1261–1264. doi:10.1038/nbt761.

Yabe, S., Alexenko, A.P., Amita, M., Yang, Y., Schust, D.J., Sadovsky, Y., Ezashi, T., Roberts, R.M., 2016. Comparison of syncytiotrophoblast generated from human embryonic stem cells and from term placentas. Proc. Natl. Acad. Sci. U.S.A. doi:10.1073/pnas.1601630113.

Yang, Y., Adachi, K., Sheridan, M.A., Alexenko, A.P., Schust, D.J., Schulz, L.C., Ezashi, T., Roberts, R.M., 2015. Heightened potency of human pluripotent stem cell lines created by transient BMP4 exposure. Proc. Natl. Acad. Sci. U.S.A. 112, E2337–E2346. doi:10.1073/pnas.1504778112.

Yu, P., Pan, G., Yu, J., Thomson, J.A., 2011. FGF2 sustains NANOG and switches the outcome of BMP4-induced human embryonic stem cell differentiation. Cell Stem Cell 8, 326–334. doi:10.1016/j.stem.2011.01.001.

Zhang, P., Li, J., Tan, Z., Wang, C., Liu, T., Chen, L., Yong, J., Jiang, W., Sun, X., Du, L., Ding, M., Deng, H., 2008. Short-term BMP-4 treatment initiates mesoderm induction in human embryonic stem cells. Blood 111, 1933–1941. doi:10.1182/blood-2007-02-074120.